

Thermal behaviour of clay mixtures with bauxite residue for the production of heavy-clay ceramics

Y. Pontikes^a, P. Nikolopoulos^b, G.N. Angelopoulos^{a,*}

^a Laboratory of Materials and Metallurgy, Department of Chemical Engineering, University of Patras, 26500 Rio, Greece

^b Laboratory of Ceramic and Composite Materials, Department of Chemical Engineering, University of Patras, 26500 Rio, Greece

Available online 19 June 2006

Abstract

“Bauxite Residue”, BR, is the main by-product of the alumina-producing Bayer cycle. Aiming at its utilisation in the production of heavy-clay ceramics, the thermal behaviour of clay body mixtures with BR was investigated. The process parameters examined were the calcite content in the clay body mixture and the firing temperature, in relation to different BR additions in the clay body mixture. The firing process was studied by means of DTA–TG and dilatometry whereas the mineralogy was determined by XRD. The DTA–TG curves did not reveal cross-reactions between body mixture and BR. However, in the mixtures with BR, sintering initiated at a lower temperature and the firing shrinkage was increased. Moreover, a second shrinkage zone was observed for high BR content and firing temperature above 950 °C, suggesting the development of a low viscosity liquid phase. The main mineralogical phases present in the BR modified mixtures after firing were quartz, hematite, clinopyroxenes, gehlenite and plagioclase. The formation of clinopyroxenes and gehlenite seems to be dependant on all process parameters examined, i.e. calcite content in the clay body mixture, BR addition and firing temperature.

© 2006 Elsevier Ltd. All rights reserved.

Keywords: Red mud; Traditional ceramics; Sintering; Bauxite Residue

1. Introduction

“Bauxite Residue”, BR, also known as “red mud”, is the main waste generated during the production of alumina by means of the Bayer cycle. It is produced during the digestion of bauxites, in a sodium hydroxide solution at elevated temperature and pressure, and leaves the cycle as a highly alkaline and of high ionic strength slurry. The solid portion consists of the insoluble compounds present in bauxites along with compounds introduced or formed during the Bayer process and a small percentage of not recovered alumina (oxy) hydroxides.¹ Its disposal remains a vital problem^{2–5} and only a few cases have been reported where the material is being utilised in industrial processes or other applications.^{6–8}

Aiming at the utilisation of BR in bulk productive industries, like in the field of traditional ceramics, the thermal behaviour of clay body mixtures with BR additions was studied. The research aims to define the reactivity of BR thus enabling the optimized design of raw materials blends and firing conditions for the pro-

duction of bricks and roofing tiles. The percentage of BR, the firing temperature, as well as the calcite content of the clay body mixture, known to have a significant impact on the mineralogical and physical-mechanical characteristics of the end bodies,⁹ were the investigated process parameters.

2. Experimental

The raw materials used were two clay body mixtures, R and W, industrially used for the production of bricks and roofing tiles, and dried BR supplied by “Aluminium of Greece”, Greece. Both body mixtures consist of quartz, calcite (Mg, Fe)-chlorite, muscovite and albite, their main difference being in the calcite and quartz content. Traces of mixed smectitic interlayer minerals, kaolinite and K-Feldspar are likely to be present whereas illite was also identified in the Carich formulation. In oxidising firing, body mixture R gives fired bodies of orange-red colour whereas body mixture W of white-cream colour. BR consists of hematite, diaspore, gibbsite, calcite, quartz, calcium aluminum iron silicate hydroxide $[\text{Ca}_3\text{AlFe}(\text{SiO}_4)(\text{OH})_8]$, perovskite $[\text{CaTiO}_3]$, cancrinite $[\text{Na}_6\text{Ca}_2\text{Al}_6\text{Si}_6\text{O}_{24}(\text{CO}_3)_2 \cdot 2\text{H}_2\text{O}]$ and; goethite and sodium aluminium silicate hydrate $[\text{Na}_2\text{O} \cdot \text{Al}_2\text{O}_3 \cdot 1.68\text{SiO}_2 \cdot 1.73\text{H}_2\text{O}]$

* Corresponding author. Tel.: +30 2610997509; fax: +30 2610990917.
E-mail address: angel@chemeng.upatras.gr (G.N. Angelopoulos).

Table 1

Chemical composition, in wt.%, of clay body mixtures W and R and of bauxite residue, BR

Material	SiO ₂	Al ₂ O ₃	CaO	Fe ₂ O ₃	MgO	K ₂ O	Na ₂ O	TiO ₂	L.O.I.	CaCO ₃
R	61.43	12.31	8.40	5.45	1.98	1.77	0.52	n.d.	7.41	13.8
W	50.34	9.11	13.19	4.91	2.04	1.98	1.66	n.d.	16.02	22.7
BR	7.79	17.04	11.64	44.34	0.57	0.07	3.17	5.12	9.77	9.70

n.d.: not determined.

seem also to be present as minor constituents. More details on the characterisation of BR can be found elsewhere.¹⁰ The chemical analysis of the clay body mixtures R and W, as well as of BR, is presented in Table 1.

For the preparation of the samples, BR was introduced at steps of 10 wt.%, replacing the clay body mixture, up to 40 wt.%. The samples were named after the clay body mixture used, which defines the first letter, and the percentage of BR introduced, denoted by the number that follows. Thermal behaviour was studied by simultaneous differential thermal analysis and thermogravimetry, DTA–TG (STA 409, Netzsch, Germany) and dilatometry (402ES, Netzsch, Germany). For DTA–TG analysis, powder samples were <125 µm and tested in static air with a heating rate of 10 °C/min. Dilatometry was performed on rods, 25 mm in length and 5 mm in diameter, in static air, with a heating and cooling rate of 3 °C/min. The samples have been taken from extruded rods, after green machining and polishing with abrasive papers. X-ray diffraction analysis (PW1830, Philips, The Netherlands) was performed on samples fired in a laboratory muffle furnace at three maximum temperatures 900, 950 and 1000 °C. The operating parameters were Cu Kα radiation, 30 mA and 40 kV, for a 2θ range from 10° to 70°. The heating rate from room temperature to 600 °C was approximately 60 °C/h, holding time at 600 °C was 2 h, from 600 °C to maximum firing temperature heating rate was 40 °C/h and 4 h soaking time. Samples were left to cool inside the furnace until room temperature. The firing temperature did not exceed 1000 °C, in view of the typical industrial conditions employed in the production of bricks and roofing tiles. In any case, firing above 1100 °C should be avoided due to the reduction of Fe³⁺ to Fe²⁺,¹¹ and the O₂ evolution that may lead to bloating.¹²

3. Results and discussion

The DTA–TG curves for R and W, with 0, 20 and 40 wt.% BR, are depicted in Figs. 1 and 2, respectively. For the mixtures with BR, the first endothermic peak corresponds to two reactions with maxima at 240 and 285 °C. It is attributed to the removal of crystalline water from calcium aluminum iron silicate hydroxide and most probably sodium aluminum silicate hydrate. At 324 °C a smooth peak appears in both R40 and W40, attributed to the decomposition of gibbsite. The decomposition of diaspore takes place at 510–540 °C;^{10,13} for R40 the endothermic hump is clearly visible whereas for W40 the peak is less intense. For a temperature higher than 700 °C, the dissociation of calcite initiates which is concluded before 800 °C. The reactions taking place at a higher temperature were not identified.

The TG curves for the studied mixtures of R with BR appear similar. A constant weight loss takes place up to 760 °C, whereas for higher temperatures a plateau is observed and only minimal weight change was recorded. The overall weight loss is practically the same for all mixtures. In the case of W, weight loss is observed up to 800 °C. For W20 and W40, the corresponding temperatures are 790 and 785 °C, respectively, in accordance to the decreasing percentage of calcite in the body. This is also reflected on the total weight loss, the less it being the less the calcite in the mixture.

The results from dilatometry are presented in Figs. 3 and 4, for R and W group of samples respectively. All mixtures show similar dilatation behaviour up to 700 °C, the main difference being the less intense quartz α ↔ β inversion in the BR modified mixtures. At a higher temperature sintering initiates accompa-

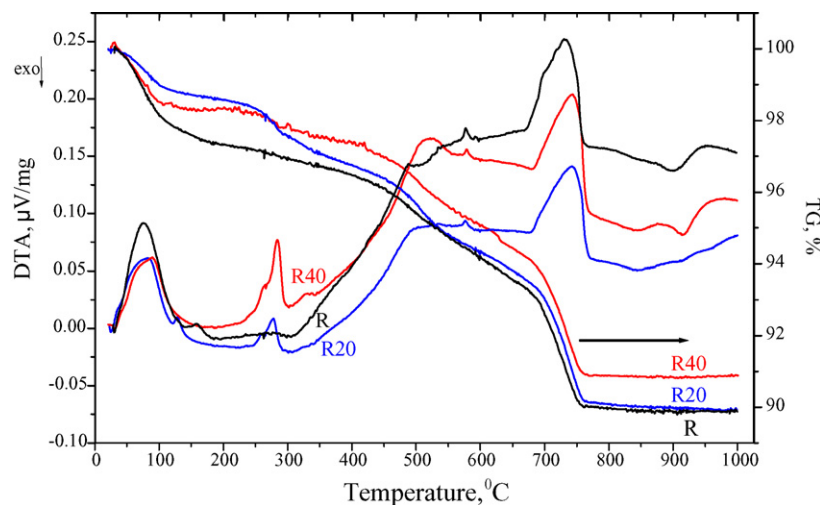


Fig. 1. DTA–TG curves for the clay body mixture R, and for the mixtures of R with 20 and 40 wt.% bauxite residue substitution, R20 and R40, respectively.

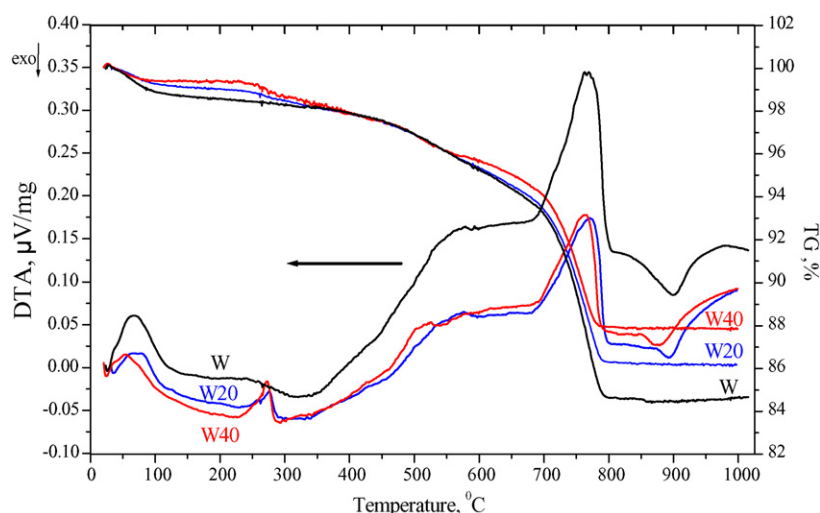


Fig. 2. DTA–TG curves for the clay body mixture W, and for the mixtures of W with 20 and 40 wt.% bauxite residue substitution, W20 and W40, respectively.

nied by abrupt shrinkage. For all formulations, the breakpoint of the curves was shifted at a lower temperature for an increasing BR content. This behaviour can be attributed to the higher specific surface of BR, approximately $11 \text{ m}^2/\text{g}$ measured by BET technique, in comparison to the body mixture, approximately $5 \text{ m}^2/\text{g}$, that enables the mass transport phenomena to take place more readily.

Shrinkage during firing was increased for both clay mixtures with BR. For the R group, shrinkage increases accordingly to the content of BR; for W group the highest shrinkage was observed for W30. Results presented elsewhere,¹⁴ for a similar to W clay body mixture with BR, demonstrate a comparable trend. In view of the relatively low sintering temperature, the different extent of firing shrinkage should be primarily linked with the packing efficiency during the formation of the samples. Experiments, not presented herein, have shown that for an increasing BR content the open porosity of the extruded green samples increases. The more open configuration leads to higher firing shrinkage but typically limits the achievement of high-density final microstructures.

After maximum densification at 900°C approximately for R mixture, further heating has a moderate effect resulting in slight expansion of the body. For the temperature interval $900\text{--}950^\circ\text{C}$, all mixtures of R with BR demonstrate a comparable dilatometric behaviour due to the similar mineralogical composition in terms of Ca-rich phases. For W, increase of the temperature beyond 890°C approximately results in expansion, as observed elsewhere for calcite-rich clay formulations.¹⁵ For the mixtures of W with BR, the expansion rate for the temperature interval $890\text{--}950^\circ\text{C}$ gradually decreases as the BR content increases. This phenomenon is related to the decreasing percentage of Ca-rich phases for an increasing BR substitution in W.

For temperatures higher than 950°C and BR percentage of 40 wt.%, a second shrinkage zone was observed for both clay body mixtures. This effect is attributed to an enhanced formation of low viscosity liquid phase. For W40, the shrinkage zone was less intense compared to R40, mainly due to the more open microstructure as a result of the higher calcite content in the raw mixture.

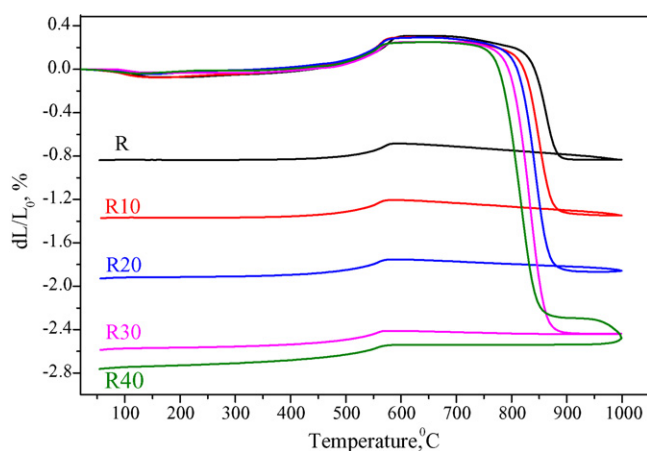


Fig. 3. Dilatometry curves for the clay body mixture R and for the mixtures of R with up to 40 wt.% bauxite residue (BR) substitution.

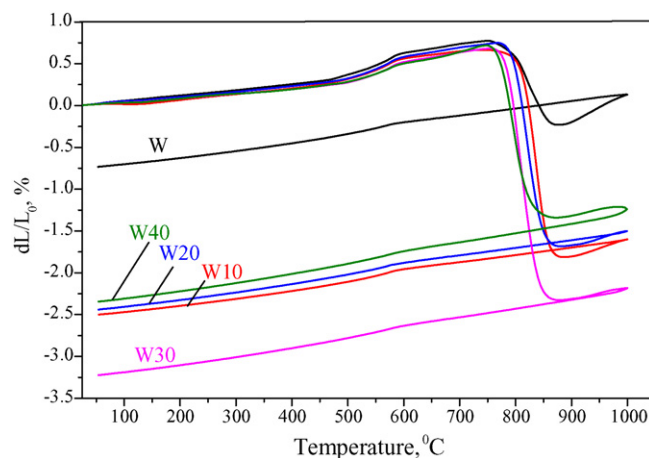


Fig. 4. Dilatometry curves for the clay body mixture W and for the mixtures of W with up to 40 wt.% bauxite residue (BR) substitution.

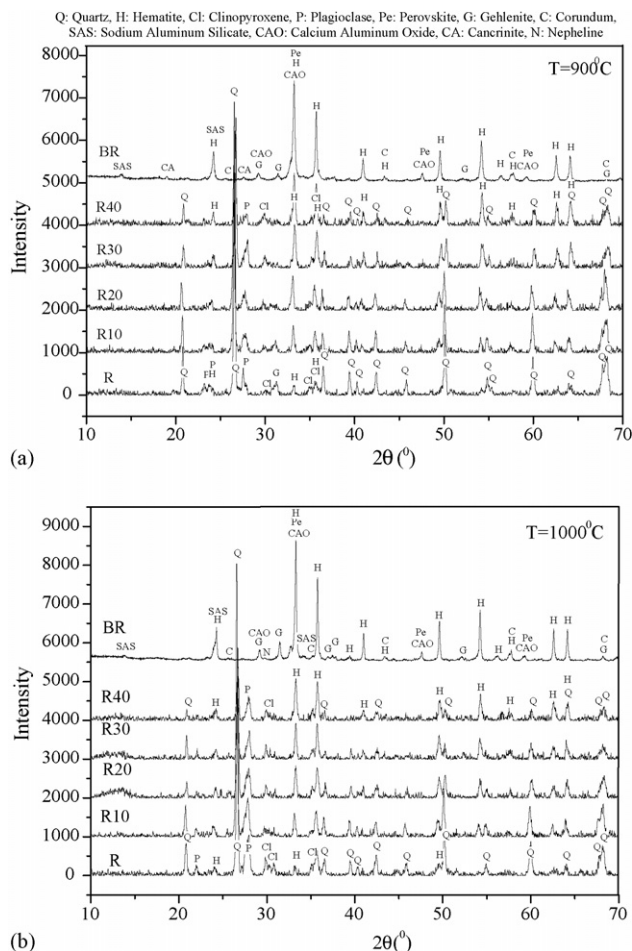


Fig. 5. XRD diagrams for the clay body mixture R and for the mixtures of R with up to 40 wt.% bauxite residue (BR) substitution. Firing took place at (a) 900 °C and (b) 1000 °C.

The results from the XRD analysis for the R group of samples and BR, fired at 900 °C, are presented in Fig. 5(a). The main phases identified for R were quartz, plagioclase, clinopyroxenes, gehlenite and hematite. In BR fired at the same temperature, hematite, perovskite, corundum, gehlenite, sodium aluminium silicate $[\text{Na}_6(\text{AlSiO}_4)_6]$ and cancrinite $[\text{Na}_6\text{Ca}_{1.5}\text{Al}_6\text{Si}_6\text{O}_{24}(\text{CO}_3)_{1.6}]$ were the phases detected; calcium aluminum oxide ($\text{Ca}_3(\text{AlO}_3)_2$) is also likely to be present. For an increasing BR content substituting the R body mixture, the peaks of hematite become more intense in view of the high concentration of BR in hematite. The peaks of quartz, gehlenite and plagioclase gradually decrease, whereas clinopyroxenes' become more intense. This is in line with the chemistry of the body mixtures being closer to clinopyroxenes structure than to gehlenite, although rarely such systems are in thermodynamic equilibrium.¹⁶

In Fig. 5(b) the results from the XRD analysis for the R group of samples and BR, fired at 1000 °C, are being presented. For R, quartz, plagioclase-probably anorthite, hematite and clinopyroxenes were the identified phases. In BR, fired at the same temperature, hematite, perovskite, corundum, gehlenite, sodium aluminium silicate $[\text{Na}_6(\text{AlSiO}_4)_6]$ and nepheline $[\text{NaAlSiO}_4]$

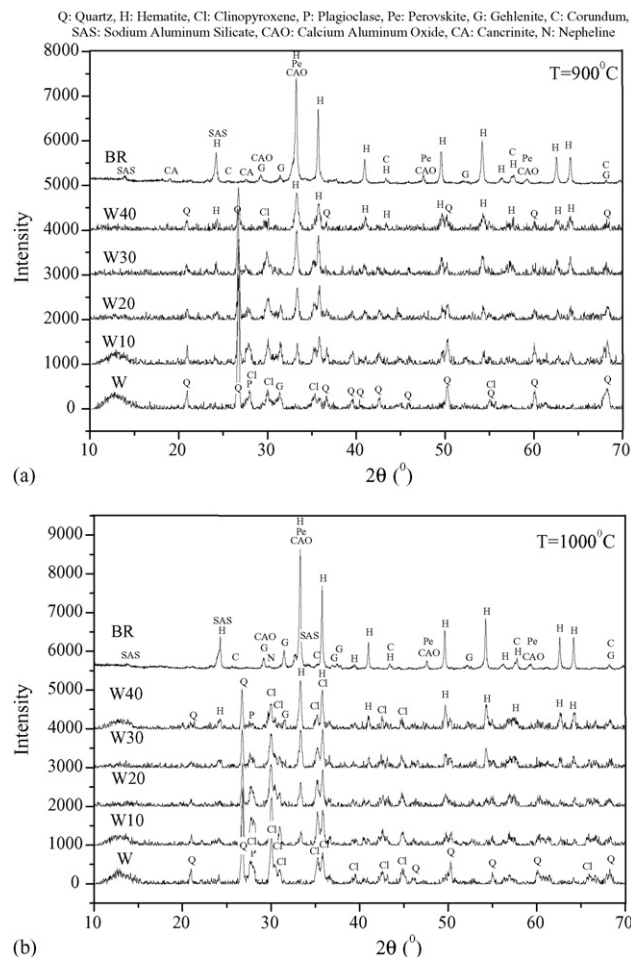


Fig. 6. XRD diagrams for the clay body mixture W and for the mixtures of W with up to 40 wt.% bauxite residue (BR) substitution. Firing took place at (a) 900 °C and (b) 1000 °C.

were detected, whereas calcium aluminum oxide ($\text{Ca}_3(\text{AlO}_3)_2$) is likely to be present. For the mixtures of R and BR, the identified phases were quartz, plagioclase, clinopyroxenes and hematite. Gehlenite has not been formed; both the chemistry of the bodies and the higher firing temperature seem to favour the formation of clinopyroxenes.

The results from the XRD analysis for the W group of samples and BR, fired at 900 °C, are presented in Fig. 6(a). For W, quartz, plagioclase, clinopyroxenes and gehlenite were identified. For an increasing substitution of W with BR, the peaks of the above phases become weaker in comparison with hematite. For 40 wt.% BR, the major phases present are quartz, hematite and clinopyroxenes. For firing at 1000 °C, a similar “diluting effect” is depicted, Fig. 6(b). However, gehlenite was detected for BR content higher than 20 wt.%. This was not anticipated in view of the high firing temperature and due to the fact that the available CaO involved in gehlenite formation, decreases with the addition of BR. The fact that gehlenite increases accordingly to the BR content (verified also for 50 wt.% BR substitution) prompts for a connection between gehlenite formation and BR. It is therefore likely that the grain size distribution of calcite

in BR plays a significant role, creating calcium rich microsites that promote the gehlenite formation.¹⁶ The role of calcite's grain size on the formation of gehlenite has been demonstrated elsewhere¹⁷ whereas XRD analysis, on different grain fractions of BR, revealed a calcite enrichment for particles $>32\text{ }\mu\text{m}$.¹⁰ This effect was not apparent in the respective R samples with BR, probably due to the moderate calcite content in the body mixture.

As a general comment on the XRD results, it can be stated that the final mineralogical composition of the mixtures appears to be an assemblage of the clay body mixture and BR. However, the interplay between clinopyroxenes and gehlenite is noteworthy. Moreover, a number of crystalline compounds present in BR have not been detected in the mixtures with clay. Although it is quite definite that a number of compounds has not reacted (i.e. corundum) and has not been detected due to analytical limitations, it seems also likely that other compounds (i.e. sodium aluminium silicate, nepheline) may have been involved in the development of liquid phase. This hypothesis is in accordance with the dilatometric data and in line with other reported works on similar systems.¹⁸

4. Conclusions

For clay body mixtures with BR, the initiation of the sintering zone took place at a lower temperature. The firing shrinkage is higher for the mixtures with BR, however does not increase in all cases accordingly with the content of BR. For BR percentage in excess of 40 wt.% and firing temperature higher than 950 °C, low viscosity liquid phase seems to be formed, as indicated by the second shrinkage zone observed in dilatometry. The final mineralogical composition of the mixtures appears to be an assemblage of the clay body mixture and BR. Nevertheless, the formation of clinopyroxenes and gehlenite seems to be dependant on all process parameters examined, i.e. calcite content in the clay body mixture, BR addition and firing temperature.

Acknowledgements

The authors acknowledge the financial support provided by the "ΕΠΙΑΝ" project no. 12252/19-11-02. Y.P. is thankful to the State Scholarship Foundation of Greece for the financial support he is receiving during his PhD study. Mr. D. Boufounos and Mr. D. Fafoutis, from "Aluminium of Greece", are also gratefully acknowledged for their contribution.

References

1. Hausberg, J., Happel, U., Meyer, F. M., Mistry, M., Röhrlich, M., Koch, H. et al., Global red mud production potential through optimised technologies and ore selection. *Miner. Resour. Eng.*, 2000, **9**(4), 407–420.
2. Thakur, R. S. and Das, S. N., *Red Mud Analysis and Utilisation*. Publications and Information Directorate and Wiley Eastern Limited, New Delhi, 1994.
3. Technology Roadmap for Bauxite Residue Treatment and Utilization. The Aluminum Association, 2000.
4. Agrawal, A., Sahu, K. K. and Pandey, B. D., Solid waste management in non-ferrous industries in India, Resources. *Conserv. Recycling*, 2004, **42**, 99–120.
5. Fortin, L., Martinet-Catalot, V. and Guimond, J., Bauxite residue enhancement projects at Alcan Arvida research & development centre: strategy and status. In *Proceedings of the Seventh International Alumina Quality Workshop*, 2005, pp. 242–245.
6. Rodríguez, G. A. P., Rivera, F. G. and De Aza Pendas, S., Manufacture of ceramic materials from Bayer process red muds. *Boletín de la Sociedad Española de Cerámica y Vidrio*, 1999, **38**(3), 220–226.
7. <http://www.redmud.org>.
8. Bott, R., Langeloh, T. and Hahn, J., Re-usage of dry bauxite residue. In *Proceedings of the Seventh International Alumina Quality Workshop*, 2005, pp. 236–241.
9. Cultrone, G., Sebastián, E., Elert, K., de la Torre, M. J., Cazalla, O. and Rodríguez-Navarro, C., Influence of mineralogy and firing temperature on the porosity of bricks. *J. Eur. Ceram. Soc.*, 2004, **24**, 547–564.
10. Pontikes, Y. T., Stivanakis, V. M., Angelopoulos, G. N., Boufounos, D., Fafoutis, D., Papageorgiou, D. and Chaniotakis, E., Characterization of dried red mud aiming at its utilization. In *Proceedings of the Fourth Pan-Hellenic Conference on Chemical Engineering*, 2003, pp. 1029–1032.
11. Sglavo, V. M., Campostrini, R., Maurina, S., Carturan, G., Monagheddu, M., Budroni, G. et al., Bauxite "red mud" in the ceramic industry. Part 1. Thermal behavior. *J. Eur. Ceram. Soc.*, 2000, **20**, 235–244.
12. Tauber, E., Hill, R. K., Crook, D. N. and Murray, M. J., Red mud residues from alumina production as a raw material for heavy clay products. *J. Aust. Ceram. Soc.*, 1971, **7**(1), 12–17.
13. Mackenzie, R., *Differential Thermal Analysis, vol. 1*. Academic Press, 1972, pp. 280–283.
14. Stivanakis, V. M., Pontikes, Y. T., Angelopoulos, G. N., Boufounos, D. and Fafoutis, D., On the utilization of the Red Mud in the heavy clay industry in Greece. In *Proceedings of the 10th Int. Cer. Congr. and Third Forum on New Mat.*, vol. 5, 2002, pp. 187–194.
15. Peters, T. and Iberg, R., Mineralogical changes during firing of calcium-rich brick clays. *Am. Ceram. Soc. Bull.*, 1978, **57**, 504.
16. Riccardi, M. P., Messiga, B. and Duminuco, P., An approach to the dynamics of clay firing. *Appl. Clay Sci.*, 1999, **15**, 393–409.
17. Okada, K., Watanabe, N., Jha, K. V., Kameshima, Y., Yasumori, A. and MacKenzie, K. J. D., Effects of grinding and firing conditions on $\text{CaAl}_2\text{Si}_2\text{O}_8$ phase formation by solid-state reaction of kaolinite with CaCO_3 . *Appl. Clay Sci.*, 2003, **23**, 329–336.
18. Sglavo, V. M., Maurina, S., Conci, A., Salviati, A., Carturan, G. and Cocco, G., Bauxite "red mud" in the ceramic industry. Part 2. production of clay-based ceramics. *J. Eur. Ceram. Soc.*, 2000, **20**, 245–252.